

Weak Measurements As an Instance of Non-Ideal Measurements¹

A. K. Pan* and A. Matzkin**

Laboratoire de Physique Théorique et Modélisation (CNRS Unité 8089), Université de Cergy-Pontoise, 95302 Cergy-Pontoise cedex, France

*e-mail: alok.pan@u-cergy.fr

**e-mail: alexandre.matzkin@u-cergy.fr

Received November 1, 2011; in final form, November 11, 2011; published online September 3, 2012

Abstract—We introduce weak measurements (WM) as a type of non-ideal measurement (NIM) coupling the system and the measuring device in a specific manner involving a weak interaction followed by post-selection. For the particular case of a WM measurement of spin, we solve the quantum dynamics for the coupled system-meter ensemble exactly for any type of non-ideal measurement. The standard WM regime is obtained as a limiting case; eccentric “semi-weak” values not only appear in other cases of NIM, but can also have a larger magnitude than the usual weak values. A couple of examples comparing the merits of the WM regime and of the exact treatment in situations of potential interest to quantum information applications are considered.

DOI: 10.1134/S1054660X12100167

1. INTRODUCTION

The issue of measurement remains to this day one of the most fundamental problems in quantum mechanics. When a measured system interacts with a measurement apparatus, the resulting state is an entangled superposition of all the available system-meter configurations. A definite measurement outcome appears in a second step, when the entangled superposition “collapses,” or becomes projected, to a single, unpredictable final system-meter configuration. For ideal measurements, the meter states in the entangled superposition are orthogonal, so that upon collapse the final meter state is unambiguously correlated with a given measured property of the system. For non-ideal measurements, the meter states are not orthogonal: after collapse reading the meter does not allow to infer unambiguously the state of the measured system.

Non-ideal measurements can easily be implemented in classical mechanics, in which case the measurement apparatus would be qualified as not fulfilling its role. The situation is different in the quantum world. Aharonov, Albert, and Vaidman (AAV) [1] introduced a scheme, baptized “weak measurement” (WM), in which only the first step of a non-ideal measurement is performed, and subsequently a second projective measurement is made. The quantum interference arising from the coherence of the meter states yields a distribution that is qualitatively different from the one obtained for ideal measurements. In particular, instead of being maximal around the eigenvalues, the maximum of the meter distribution indicates a

“weak value” that is generally different, and sometimes considerably larger, than any eigenvalue. Investigations dealing with WM have gained a significant and increasing interest, not only from a theoretical perspective [2–13], but also in experimental works [14–22].

The original AAV treatment, that has since then been applied the most frequently, is based on an approximate limiting case for weak couplings and nearly overlapping device states. This allows to employ a first order asymptotic expansion, yielding an approximate but compact expression for the weak value of the measured operator. However WMs can be derived, from a more general standpoint, as a particular instance of non-ideal measurements followed by a post-selection. This approach is particularly advantageous when the Schrödinger equation describing the evolution of the coupled system-measurement device ensemble can be solved exactly, as the pointer distribution can then be obtained exactly.

Moreover there are situations in which the AAV treatment breaks down due to its approximate nature. This is why very recently several works [9–11] have attempted to go beyond the first order expansion.

In this paper we will describe an exact approach for WMs of spins. We will see in particular that the exact approach can be useful when applications to quantum information are considered. Indeed the original WM treatment has some defects (unitarity not preserved, weak values undefined for orthogonal initial and post-selected states...) that can be remedied when an exact treatment can be performed. In Section 2 we will give a general overview concerning non-ideal measurements. WMs will be introduced in this context. In Sec-

¹ The article is published in the original.

tion 3 we revisit the AAV approach for WMs of spins and compare it to an exact treatment based on solving the Schrödinger equation. We will see that for an arbitrary non-ideal measurement apparatus one can define “semi-weak values” that approach the usual weak values in the asymptotic limit. In Section 4 we will point out some ambiguities of the usual WM treatment in situations that may be of interest in quantum information applications. We also give an example in which the exact treatment allows to find a solution to a quantum game that would be impossible to solve with the usual approach. Our conclusions will be given in Section 5.

2. NON-IDEAL MEASUREMENTS

2.1. Classical Measurements

Measurements in classical mechanics are more involved than the straw man generally presented when contrasting the classical and quantum measurement processes. The initial state of a system is seldom a point but a distribution $\rho_S(\mathbf{x}, \mathbf{p}, t_i)$ in phase space. The measurement apparatus has a distribution $\rho_M(\mathbf{X}, \mathbf{P}, t_i)$. The evolution of ρ_S and ρ_M is generated by a Hamiltonian of the type

$$H_0(\mathbf{x}, \mathbf{p}) + g(t)A(\mathbf{x}, \mathbf{p})\mathbf{X}, \quad (1)$$

where for definiteness we assume the measured system variable $A(\mathbf{x}, \mathbf{p})$ couples to the X coordinate of the meter with a strength and during the short time-window specified by $g(t)$. H_0 is the Hamiltonian of the system and the meter is assumed initially at rest. It is straightforward [23] to solve the equations of motion: the meter will acquire a momentum P_X proportional to $\int g(t')A(\mathbf{x}, \mathbf{p})dt'$. The system will be disturbed by the measurement: *any* dynamical variable $B(\mathbf{x}, \mathbf{p})$ will undergo a backreaction due to the interaction with the meter. The precision ΔA to which the measurement outcome can be known depends on the meter distribution.

Assume, for the sake of comparison with the quantum situation, that ρ_S is such that A is narrowly peaked around two values, $A = \pm 1$. The phase-space distribution after the measurement is formally obtained by solving the Liouville equation. Integrating the phase-space distribution over the momenta \mathbf{p} and \mathbf{P} of the system and the device respectively leads to the configuration space distribution

$$\rho_S^+(\mathbf{x}, t)\rho_M^+(\mathbf{X}, t) + \rho_S^-(\mathbf{x}, t)\rho_M^-(\mathbf{X}, t), \quad (2)$$

where the \pm superscripts label the motion of the meter in the positive or negative directions along X , according to whether the value of A was around ± 1 . If one reads the meter by looking at its position \mathbf{X}_y —for example when the meter hits a screen placed perpendicularly to the initial direction prior to the measure-

ment—then the measurement will be said to be *ideal* if \mathbf{X}_y can be ascribed unambiguously either to ρ_M^+ or to ρ_M^- . The condition for the measurement to be ideal is thus that the statistical distributions ρ_M^\pm of Eq. (2) do not overlap in configuration space. If the distributions do overlap, then the measurement will be said to be *non-ideal*: a reading of the meter does not correlate with a specific value of the measured system variable. Without developing a specific model to get quantitative estimates, it is clear that the idealness of the measurement will depend on the initial distribution of the meter (a broad initial distribution is unlikely to yield two separate post-measurement distributions) and on the coupling strength (a small coupling strength will not lead to momenta P_X sufficiently large so as to lead to a total separation).

Note that with the Hamiltonian given by Eq. (1) the value of the measured property $A(\mathbf{x}, \mathbf{p})$ at the time of measurement is perfectly well-defined (including the disturbance it suffers). The use of statistical distributions is due to the ignorance of the precise initial conditions of the system and measuring device variables. The distribution given by Eq. (2) is epistemic (see, for example [26]) and is updated once the outcome is *known* (irrespective of whether the measurement took place a few nanoseconds or a few centuries ago). In the ideal case the distribution given by Eq. (2) is updated to a new distribution that is contained within one of the two terms of Eq. (2), depending on the outcome. In the non-ideal case, Eq. (2) is updated to a new distribution still containing terms associated with both outcomes; the form of the updated distribution depends on the specific form of Eq. (2) and on the precision of the measurement.

2.2. Quantum Measurements

The corresponding quantum version of the classical measurement scheme depicted above involves an initial state at $t = t_i$

$$|\Psi(t_i)\rangle = |\chi(t_i)\rangle_S |\psi(t_i)\rangle_M, \quad (3)$$

where $|\chi(t_i)\rangle$ and $|\psi(t_i)\rangle$ denote quantum states of the system and meter respectively at $t = 0$. The coupling Hamiltonian is taken of the form

$$\hat{H}_{\text{int}} = g(t)\hat{A}\hat{X}, \quad (4)$$

where \hat{A} is the operator representing the measured property of the system having eigenstates $|\alpha_\pm\rangle$ with eigenvalues ± 1 . The expansion of $|\chi(t_i)\rangle$ over this basis reads

$$|\chi(t_i)\rangle = \alpha_+|\alpha_+\rangle + \alpha_-|\alpha_-\rangle. \quad (5)$$

$g(t)$ is again a window function non-vanishing only during the duration τ of the interaction; we shall define

the overall measurement strength by $\bar{g} = \int_{\Delta t' = \tau} g(t') dt'$. If the interaction is turned on at $t_i = 0$, then for $t > \tau$ the unitary evolution brings $|\Psi_0\rangle$ to

$$|\Psi(t)\rangle = \alpha_+ |\alpha_+\rangle |\psi_+(t)\rangle + \alpha_- |\alpha_-\rangle |\psi_-(t)\rangle. \quad (6)$$

This entangled superposition subsists until the second stage of the measurement is completed, that is until the meter collapses to a final state, actualizing at that point the state of the system.

For ideal measurements the meter states $|\psi_+(t)\rangle$ and $|\psi_-(t)\rangle$ are orthogonal, establishing a one to one correspondence with the system states. If the spatial position \mathbf{X}_f of the meter is monitored, the recording of an event at this position implies that either $\langle \mathbf{X}_f | \psi_+ \rangle$ or $\langle \mathbf{X}_f | \psi_- \rangle$ vanish, depending on \mathbf{X}_f . The meter has collapsed to a subspace of $|\psi_+(t)\rangle$ and $|\psi_-(t)\rangle$ each correlated unambiguously with $A = +1$ and $A = -1$, respectively. The measurement process is completed at that point [24, 25]; it is mathematically equivalent to the projection $\langle \alpha_{\pm} | \chi(t_i) \rangle$. Whether this collapse is physically real [26] or an epistemic operation (as is the case for the classical distributions mentioned above) lies at the heart of the measurement problem [27]. A purely epistemic approach assimilating the collapse with a Bayesian update is hardly tenable, as this would imply that the system possessed the measured property prior to the collapse. On the other hand, attempts to understand what collapses and why it collapses remain highly controversial and many solutions have been proposed (dynamical reduction models implying spontaneous collapse [28], the need to place a quantum-classical cut when the quantum measurement is amplified in an ultimately classical device [29], the irreversibility of the phase delocalization when the meter interacts with the high number of degrees of freedom of its environment [30], the existence of a point-like particle populating a single term of the superposition whereas the other wavepackets are empty [31], our biological inability to follow the simultaneous branches of an infinity of multiple universes [32], etc.).

In the non-ideal case, the device states are *not* orthogonal. The collapse brings the meter to a common subspace of $|\psi_+(t)\rangle$ and $|\psi_-(t)\rangle$ and the resulting meter distribution displays the coherence of the overlapping device states. The basis ambiguity does not allow the measurement process to yield a definite outcome for the measured property of the system, and there is thus no one to one correspondence between the system and the pointer position. Nevertheless, non-ideal measurements can be useful when an additional ideal projective measurement is made subsequently to the non-ideal one: for historical reasons related to attempts to give a time-symmetric formulation of quantum mechanics [33], the selection of a given eigenstate of this additional measurement is known as post-selection.

2.3. Invoking Post-Selection: Exotic Meter Distributions and “Weak Measurements”

For $t > \tau$, we have seen that the system-meter state is entangled and given by Eq. (6). Now, before completing the last step of that measurement (with the irreversible amplification that would lead to the collapse of the system-meter entangled state), a complete ideal measurement (i.e., including collapse) is made for a different property of the system, represented by the operator \hat{B} having eigenstates $|\beta_{\pm}\rangle$ with eigenvalues ± 1 . A given final state among the two possible outcomes, say, $|\beta_+\rangle$ is selected. The projection $\langle \beta_+ | \Psi(t) \rangle$ yields (it is unnecessary, though straightforward, to introduce explicitly the second meter states) the non-ideal meter state

$$|\psi_M^{\text{ps}}\rangle = \alpha_+ \langle \beta_+ | \alpha_+ \rangle |\psi_+(t)\rangle + \alpha_- \langle \beta_+ | \alpha_- \rangle |\psi_-(t)\rangle. \quad (7)$$

Hence after post-selection the first measuring device—the one that was employed for the non-ideal measurement, will be described by the non-diagonal density matrix

$$\rho_M^{\text{ps}} = \text{Tr}_S(\Pi_{\beta_+} |\Psi(t)\rangle \langle \Psi(t)| \Pi_{\beta_+}), \quad (8)$$

where $\Pi_{\beta_+} \equiv |\beta_+\rangle \langle \beta_+|$. Given that the measurement is non-ideal and that the collapse happens for a different subsequent projective measurement the meter distribution obtained from Eqs. (7), (8) is different from the one associated with ideal measurements (non-overlapping meter states and collapse). These distributions are not peaked at the eigenvalues but can present any form (including exotic ones, with maxima well beyond the eigenvalues) depending on the initial meter state and on the details of the measurement interaction.

A particularly interesting instance of Eqs. (7), (8) arises when the coupling interaction given by Eq. (4) is weak and the device states are nearly orthogonal: this is the weak measurement regime. The evolution operator obtained from \hat{H}_{int} can then be approximately expanded to first order with the meter state barely affected by the coupling while the system state undergoes a first order transition. As a result of the post-selection Eq. (7) can be approximated by

$$|\psi_M^{\text{ps}}(t > \tau)\rangle \approx \exp\left(i\bar{g} \left\{ \frac{\langle \beta_+ | \hat{A} | \chi(t_i) \rangle}{\langle \beta_+ | \chi(t_i) \rangle} \right\} \hat{X}\right) |\psi(t_i)\rangle, \quad (9)$$

yielding an overall phase-shift in the X variable. The term between $\{.. \}$ is the “weak value” introduced by AAV [1] which can be beyond the eigenvalue limit, whose treatment is recalled immediately below in the case of spin measurements.

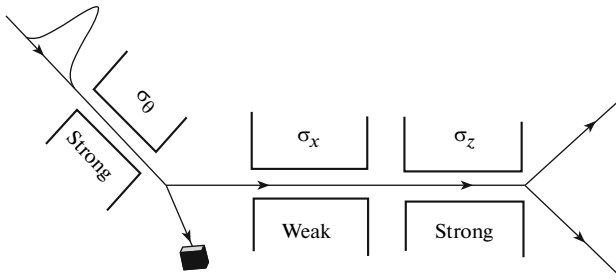


Fig. 1. Three SG setups account for the state-preparation (pre-selection), the weak measurements of the spin operator $\hat{\sigma}_x$ and the post-selection.

3. WEAK MEASUREMENT OF A DICHOTOMIC SPIN OBSERVABLE: AN EXACT TREATMENT

3.1. General Remarks

The goal is to present the WM scenario as an instant of general non-ideal measurements when the coupling is very weak representing extreme non-ideal situation. The opposite extreme limit corresponds to the strong measurement. However, between these two limiting cases there is a whole continuous range of non-ideal situations. Note that the AAV formulation of WM scenario considers only the first order expansion of the interaction and as such cannot accommodate an arbitrary non-ideal regime. We investigate these regimes in a simple analytically tractable system of spin-1/2 particle passing through a series of Stern–Gerlach setups.

It is the feature of this exact treatment allows us to explore the intermediate non-ideal regimes of measurement situations where the corresponding measured values we coin as “semiweak” values that display potentially interesting effects. We will show in particular that in the non-ideal regime, not only can eccentric outcomes be obtained, but that the resulting semiweak values can also be beyond the weak value predicted by AAV formalism. Interestingly, when the standard AAV formalism fails for orthogonal pre- and post-selection, we will also see that it is indeed possible to observe dichotomic outcomes of the pointer, as in the case of strong measurements, but with eccentric shifts.

We shall first briefly encapsulate the essence of the standard WM of AAV and point out its limitations. We then generalize the treatment for any arbitrary strength of the coupling that requires the relevant Schrödinger equation to be exactly solved.

The standard WM procedure [1, 2] comprises three different measurements: a strong measurement for state preparation (historically termed as pre-selection), a strong projective measurement for selecting a specific subensemble (coined as post-selection), and in between the pre- and post-selection a weak interaction is introduced so that system state remains virtually unaffected by this intermediate interaction (see Fig. 1)

allowing a nearly overlapping meter states. The entire process can be explained in terms of a series of three Stern–Gerlach (SG) setups—the problem that can be solved analytically.

Let a beam of spin 1/2 neutral particles, pass through these SG setups. The first SG is used to prepare the spin pre-selected state labeled by $|\chi_{in}\rangle$. The total initial wave function after the first SG setup is $\Psi_{in} = \psi_0(x)|\chi_{in}\rangle$. The spatial part $\psi_0(x)$ is taken to be a Gaussian wave packet peaked at the entry point ($x = 0$) of the second SG at $t = 0$. The Fourier transform of $\psi_0(x)$ in momentum space is $\phi_0(p_x)$.

The particles having the state $\Psi_{in} = \psi_0(x)|\chi_{in}\rangle$ then pass through the second SG setup that is used for measuring a spin observable, say, $\hat{\sigma}_x$. The interaction Hamiltonian is given by $H = f(t)\mu\hat{\sigma} \cdot \mathbf{B}$, where $\mathbf{B} = (bx, 0, 0)$ and μ is the magnetic moment of neutron. $f(t)$ is a smooth function of t vanishing outside the interval $0 < t < \tau$ and obeying $\int_0^\tau f(t)dt = \tau$, where τ is the transit time during which the neutrons interact with the magnetic field. The total state after the interaction can then be written as

$$\Psi' = e^{-\frac{i\mu b\tau x \hat{\sigma}_x}{\hbar}} \psi_0(x)|\chi_{in}\rangle. \quad (10)$$

3.2. The Standard Approach

Now, if the magnetic field and transit time are taken to be very small, the interaction can be considered to be weak. Then the exponential in Eq. (10) can be approximated to the first order neglecting higher order terms. This is exactly what is done in the standard AAV treatment. After the weak interaction, a strong projective measurement is performed by using the third SG setup and the particles are “post-selected” in a definite final spin state $|\chi_f\rangle$ which allows to finally write the device state as

$$\psi_f(x) = \langle \chi_f | \chi_{in} \rangle e^{-\frac{i\mu b\tau x}{\hbar} (\sigma_x)_w} \psi_0(x), \quad (11)$$

where

$$(\sigma_x)_w = \frac{\langle \chi_f | \sigma_x | \chi_{in} \rangle}{\langle \chi_f | \chi_{in} \rangle} \quad (12)$$

is known as weak value of the observable $\hat{\sigma}_x$. The derivation of the Eq. (11) and proper conditions to neglect the higher order terms of $b\tau$ in obtaining Eq. (12) can be found, for example, in [11].

The final momentum distribution can then be written as

$$|\phi_f(p_x)|^2 = |\langle \chi_f | \chi_{in} \rangle|^2 |\phi_0(p_x - p'_x(\sigma_x)_w)|^2, \quad (13)$$

where $|\langle \chi_f | \chi_{in} \rangle|^2$ is the probability of successful post-selection and $p'_x = \mu b \tau$. Note that, the final pointer position in momentum space is shifted by an amount $(\sigma_x)_w p'_x$ while in strong measurement the expected shift are $\pm p'_x$, corresponding to the eigenvalues ± 1 of $\hat{\sigma}_x$. Note that, $(\sigma_x)_w$ can be very large depending upon the pre- and post-selection.

For example, if $|\chi_{in}\rangle = |\uparrow\rangle_0 = \cos\frac{\theta}{2}|\uparrow_z\rangle + \sin\frac{\theta}{2}|\downarrow_z\rangle$ and $|\chi_f\rangle = |\uparrow\rangle_z$, then from Eq. (12) we obtain $(\sigma_x)_w = \tan\theta/2$ which tends to infinity if θ tends to $\pi/2$.

Note that, the standard WM involves a drastic approximations which is valid only for very weak coupling and the extension of this approach to the intermediate or strong regimes of coupling is not possible. These intermediate non-ideal regimes that can be referred as ‘‘semi-weak’’ situations are considered in the following Section that requires the exact solutions of the relevant Schrödinger equations involved in the setup.

3.3. Exact Treatment

We first give the exact solution for a non-ideal SG setup, that is solving the coupled Schrödinger equations for a wave packet of a spin 1/2 particle without making any specific assumptions for the coupling strength and the device states. In order to quantify the strength of a given measurement we introduce a crucial quantity is the overlap I of the wave packets (recall the wave packets play here the role of the device states). The value of I is bounded by 0 and 1, so that $I \rightarrow 0$ yields the strong ideal measurement regime, while $I \rightarrow 1$ corresponds to the standard WM scheme. Any other value of I corresponds to non-ideal measurements. We shall illustrate different types of behavior of the pointer indicating one or several semi-weak values, semiweak values beyond or between the eigenvalues, exact weak values for orthogonal pre- and post-selection.

3.3.1. Schrödinger equations. Following the same setup given by Fig. 1 we consider that the initial spin state is given by omitting the state preparation procedure. Let us consider a beam of particles, passing through the second SG setup be represented by the total wave function

$$\Psi(\mathbf{x}, t = 0) \equiv \psi_0(\mathbf{x})|\uparrow\rangle_0, \quad (14)$$

where $|\uparrow\rangle_0$ is the initial state of the system (i.e., the spin). The spatial wave function $\psi_0(\mathbf{x})$ corresponds to a Gaussian wave packet which is initially peaked at $\mathbf{x} = 0$ at $t = 0$, given by

$$\psi_0(\mathbf{x}) = \frac{1}{(2\pi\delta^2)^{3/4}} \exp\left(-\frac{\mathbf{x}^2}{4\delta^2} + i\frac{p_y y}{\hbar}\right), \quad (15)$$

where δ is the initial width of the wave packet. The wave packet moves along the $+y$ axis with the initial momentum p_y (see Fig. 1). The inhomogeneous magnetic field² $\mathbf{B} = (bx, 0, 0)$ is directed along the x -axis and confined between $y = 0$ and $y = d$. The interaction Hamiltonian is $H_i = \mu \hat{\sigma} \cdot \mathbf{B}$ where as above μ is the magnetic moment of the neutron. As the wave packet propagates through the SG magnet, in addition to the $+y$ axis motion, the particles gain momentum along $\pm x$ -axis due to the interaction of their spins with the field. Similar to Eq. (6), the system-device entangled state at τ is given by

$$\Psi(\mathbf{x}, \tau) = \alpha_+ \psi_{+x}(\mathbf{x}, \tau) \otimes |\uparrow\rangle_x + \alpha_- \psi_{-x}(\mathbf{x}, \tau) \otimes |\downarrow\rangle_x, \quad (16)$$

where the device states $\psi_{+x}(\mathbf{x}, \tau)$ and $\psi_{-x}(\mathbf{x}, \tau)$ are the two components of the spinor $\psi = \begin{pmatrix} \psi_+ \\ \psi_- \end{pmatrix}$ which sat-

isfies the Pauli equation and $\alpha_+ = \frac{1}{\sqrt{2}}\left(\cos\frac{\theta}{2} + \sin\frac{\theta}{2}\right)$

and $\alpha_- = \frac{1}{\sqrt{2}}\left(\cos\frac{\theta}{2} - \sin\frac{\theta}{2}\right)$. The reduced density matrix of the system in the x -basis representation can be written as

$$\rho_s = \begin{pmatrix} \alpha^2 & \alpha\beta I \\ \alpha\beta I^* & \beta^2 \end{pmatrix}, \quad (17)$$

where I is the overlap

$$I = \int_V \psi_{+x}^*(\mathbf{x}, \tau) \psi_{-x}(\mathbf{x}, \tau) d^3x \quad (18)$$

that quantifies the weakness of the measurement. The inner product I is in general complex but here in our case I is always real and positive. The value of the I can range from 0 to 1 depending upon the choices of the relevant parameters, such as, the magnitude of the magnetic field (b), the width of the initial wave packet (δ) and the transit time through the field region within the SG setup (τ). We calculate the analytical expressions of $\psi_{+x}(\mathbf{x}, \tau)$ and $\psi_{-x}(\mathbf{x}, \tau)$ by solving relevant Schrödinger equations.

² This form of magnetic field is unphysical as it does not satisfy the Maxwell equation $\nabla \cdot \mathbf{B} = 0$. We need at least another component to make it divergence free [34]. However on average the effect of these additional field components can be neglected under proper circumstances, resulting in this effective field usually found in textbooks and also employed in [1, 13].

The two-component Pauli equation for ψ_{+x} and ψ_{-x} can then be written

$$i\hbar \frac{\partial \psi_{+x}}{\partial t} = -\frac{\hbar^2}{2m} \nabla^2 \psi_{+x} + \mu b x \psi_{+x}, \quad (19)$$

$$i\hbar \frac{\partial \psi_{-x}}{\partial t} = -\frac{\hbar^2}{2m} \nabla^2 \psi_{-x} - \mu b x \psi_{-x}. \quad (20)$$

The solutions of the above two equations at $t = \tau$ upon exiting the SG are as follows (for a detailed derivation, see [34])

$$\begin{aligned} \psi_{+x}(\mathbf{x}; \tau) &= \frac{1}{(2\pi\delta^2)^{\frac{3}{4}}} \\ &\times \exp\left[-\frac{z^2 + \left(y - \frac{p_y\tau}{m}\right)^2 + \left(x - \frac{p_x\tau}{2m}\right)^2}{4\delta^2}\right] \\ &\times \exp\left[i\left\{-\Delta + \left(y - \frac{p_y\tau}{2m}\right)\frac{p_y}{\hbar} + \frac{p_x x}{\hbar}\right\}\right], \end{aligned} \quad (21)$$

$$\begin{aligned} \psi_{-x}(\mathbf{x}; \tau) &= \frac{1}{(2\pi\delta^2)^{\frac{3}{4}}} \\ &\times \exp\left[-\frac{z^2 + \left(y - \frac{p_y\tau}{m}\right)^2 + \left(x + \frac{p_x\tau}{2m}\right)^2}{4\delta^2}\right] \\ &\times \exp\left[i\left\{-\Delta + \left(y - \frac{p_y\tau}{2m}\right)\frac{p_y}{\hbar} - \frac{p_x x}{\hbar}\right\}\right], \end{aligned} \quad (22)$$

where $\Delta = \frac{p_x^2 \tau}{6m\hbar}$, $p_x' = \mu b \tau$, and the spreading of the wave packet is neglected throughout the evolution.

Here $\psi_{+x}(\mathbf{x}, \tau)$ and $\psi_{-x}(\mathbf{x}, \tau)$ representing the spatial wave functions at τ correspond to the spin states $|\uparrow\rangle_x$ and $|\downarrow\rangle_x$ respectively, with the average momenta $\langle \hat{p} \rangle_\uparrow$ and $\langle \hat{p} \rangle_\downarrow$, where $\langle \hat{p} \rangle_{\uparrow\downarrow} = (\pm p_x', p_y, 0)$. Within the magnetic field the neutrons gain the same magnitude of momentum $p_x' = \mu b \tau$ but the directions are such that the particles with eigenstates $|\uparrow\rangle_x$ and $|\downarrow\rangle_x$ get the drift along $+x$ -axis and $-x$ -axis respectively, while the y -axis momenta remain unchanged.

From these analytical expressions of $\psi_{+x}(\mathbf{x}, \tau)$ and $\psi_{-x}(\mathbf{x}, \tau)$ given by Eqs. (21) and (22) it is straightfor-

ward to compute the inner product I [Eq. (18)] given by

$$I = \exp\left(-\frac{\mu^2 b^2 \tau^4}{8m^2 \delta^2} - \frac{2\mu^2 b^2 \tau^2 \delta^2}{\hbar^2}\right), \quad (23)$$

which explicitly depends upon the choices of the parameters b , δ , and τ .

Now, in order to post-select the particles in the state $|\uparrow\rangle_z$ we consider immediately after the wavepacket exits the second SG setup a subsequent strong measurement of the spin observable $\hat{\sigma}_z$. In principle, the knowledge of the exact solutions allow to treat the strong and weak SG measurements on the same footing. But, as observed earlier the explicit description of this strong measurement in terms of meter states is equivalent to the usual projection and thus omitting here. Projecting $\langle \uparrow_z |$ and integrating out the y and z components of the wavepacket as they do not play any significant role (see, [11]); yields

$$\psi_{\text{post}}(x, \tau) = \frac{1}{\sqrt{2}} [\alpha_+ \psi_{+x}(x, \tau) + \alpha_- \psi_{-x}(x, \tau)]. \quad (24)$$

The corresponding momentum space wave function is

$$\phi_{\text{post}}(p_x, \tau) = \frac{1}{\sqrt{2}} [\alpha_+ \phi_{+x}(p_x, \tau) + \alpha_- \phi_{-x}(p_x, \tau)], \quad (25)$$

where $\phi_{\pm x}$ are obtained by taking the Fourier transform of Eqs. (21), (22) leaving out the y and z dependent parts, yielding,

$$\begin{aligned} \phi_{\pm x}(p_x, \tau) &= \phi_0(p_x \mp p_x') \\ &\times \exp\left(-\frac{i p_x^2 \tau}{2m\hbar} \pm \frac{i p_x p_x' \tau}{2m\hbar} - \frac{i \mu^2 b^2 \tau^3}{6m\hbar}\right), \end{aligned} \quad (26)$$

where with $\phi_0(p_x)$ is the initial momentum wave function.

The post-selected momentum wave function given by Eq. (25) is general in that no restriction on the coupling constant or on the width of the probe states have been introduced. We can now look at the device's momentum distribution in different regimes that will be characterized by the value of I .

3.3.2. Strong measurement limit: $I \approx 0$. Let the relevant parameters (b , δ , and τ) are so chosen so that $I \rightarrow 0$. In this case there is no common subspace for $\psi_{+x}(p_x, \tau)$ and $\psi_{-x}(p_x, \tau)$: each of the corresponding distributions is correlated with $\hat{\sigma}_x = +1$ and -1 respectively (see Fig. 2a).

3.3.3. Standard weak measurement limit: $I \approx 1$. The opposite limiting situation of strong measurement is WM—the extreme case of non-ideal measurement. We can choose the above parameters such that $I \approx 1$ is obtained, i.e., $\psi_{+x}(p_x, \tau)$ and $\psi_{-x}(p_x, \tau)$ are nearly same implying the coherence in the system is mostly unaffected. There is hardly any correspondence between

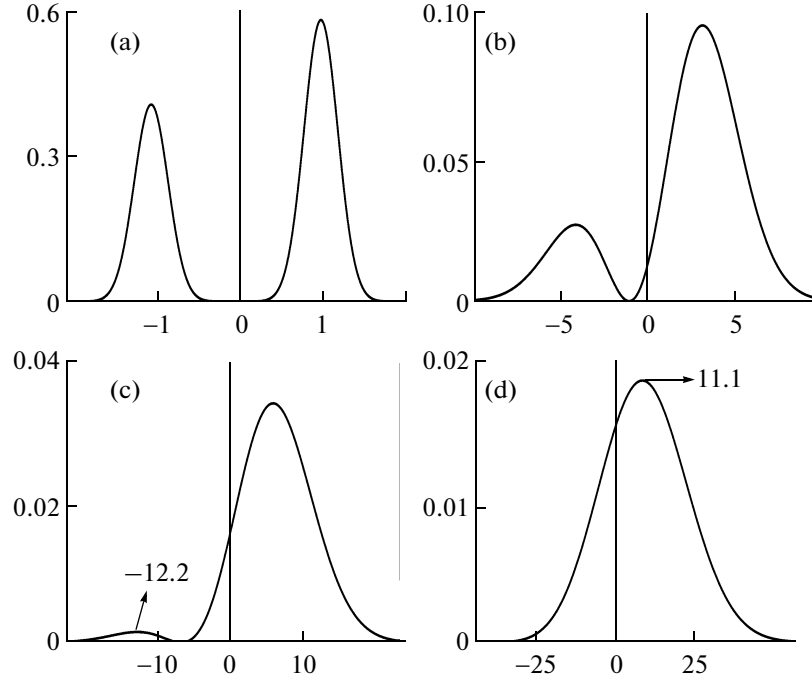


Fig. 2. The momentum distribution $|\phi_{\text{post}}(p_x, \tau)|^2$ (Eq. (25)) is plotted for four different values of the inner product (I) depending upon the suitable choices of the parameters. Here, (a, d) represents the strong and weak measurements, and (b, c) correspond the semiweak measurement situations. The weak value is $(\sigma_x)_w = 11.1$ for $\theta = 169^\circ$.

the system and the device states. A simple calculation shows that this is WM scheme proposed by AAV. For this, let us start with the pointer position space wave function given by Eqs. (21), (22) since the coupling is employed between the spin and the position variable. If the parameters b and τ are sufficiently small the value of I could be close to unity for a fixed δ and then the higher order terms of $b\tau$ can be neglected keeping only first order term. We can then write the states $\Psi_{\pm x}(\mathbf{x}; \tau)$ given by Eqs.(21), (22) as follows

$$\Psi_{\pm x}(x; \tau) \approx \Psi_0(x)(1 \pm ip'_x x/\hbar). \quad (27)$$

In this limit Eq. (24) becomes

$$\Psi_{\text{post}}(x, \tau) \approx \frac{\Psi_0(x)}{\sqrt{2}} [\alpha_+(1 + ip'_x x/\hbar) + \alpha_-(1 - ip'_x x/\hbar)].$$

Putting the values of α_+ and α_- , and simplifying we get

$$\Psi_{\text{post}}(x, \tau) \approx \cos \frac{\theta}{2} \Psi_0(x) \exp\left(ip'_x x \tan \frac{\theta}{2} / \hbar\right). \quad (28)$$

The Fourier transform of Eq. (28) gives the pointer wave function in momentum space yielding the distribution

$$|\phi_f(p_x)|^2 \approx \cos^2 \frac{\theta}{2} \left| \phi_0\left(p_x - p'_x \tan \frac{\theta}{2}\right) \right|^2 \quad (29)$$

which exactly matches the Eq. (13) of the standard WM formulation identifying $\cos^2 \frac{\theta}{2}$ and $\tan \frac{\theta}{2}$ as post-selection probability and weak value respectively, depicted in Fig. 2d.

3.3.4. Non-Ideal Measurement and the “Semi-Weak” Regime: $0 < I < 1$. The AAV formalism cannot accommodate the measurement of general non-ideal situation. When the value of I lies in the intermediate range $0 < I < 1$ a partial coherence is present in the meter states therefore displaying an interference between the overlapping meter wavefunctions. Since the pointer behavior depends on the resultant interference, by monitoring I , eccentric pointer shifts that we call “semiweak values” can be obtained in this intermediate range. Depending on the resulting interference, the pointer distribution can have two maximum, one of which can be beyond the standard weak value derived from Eq. (12). From Fig. 2c, it can be seen that the distribution is peaked at -12.2 but the weak value is 11.1 . Other behaviors of the pointer can be obtained, in particular profiles with two maxima, similar to the two peaks that characterize the strong limit, but with the maxima shifted far from the eigenvalues (Fig. 2b).

3.3.5. Exact weak values. As mentioned earlier that standard AAV formalism has a limitation that when the pre- and post-selected states are orthogonal the weak value given by Eq. (12) is undefined. This undefiniteness stems from partially expanding the exponen-

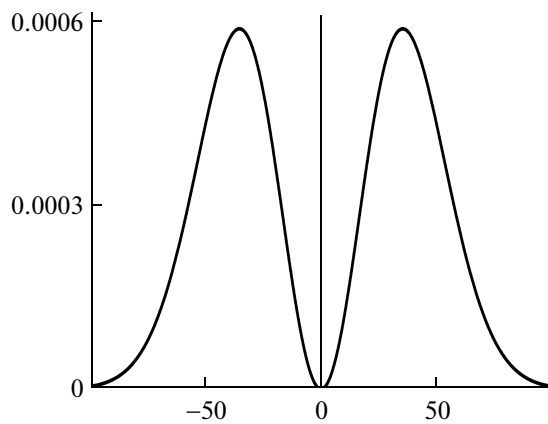


Fig. 3. The momentum distribution $|\phi_{\text{post}}(p_x, \tau)|^2$ (Eq. (30)) is plotted when $I \approx 1$ but the pre- and post-selected states are orthogonal—a situation in which the standard weak value is undefined.

tial after the post-selection. However, following our treatment we found that even in the WM regime when $I \approx 1$, pointer shifts can be obtained leading to the exact weak values. In this situation, the post-selected meter state in momentum space is given by

$$\phi_{\text{post}}(p_x, \tau) = \frac{1}{\sqrt{2}}[\phi_{+x}(p_x, \tau) - \phi_{-x}(p_x, \tau)]. \quad (30)$$

Figure 3 shows the exact meter momentum distribution for orthogonal pre and post-selected states, for parameters near the $I \approx 1$ limit. A shifted distribution displaying an eccentric maximal value—the “exact” weak value—of the type usually encountered in the WM limit, can be observed. Note that the exact weak value is perfectly finite whereas from the definition given by Eq. (12) one might be tempted to conclude (incorrectly as this would violate the conditions under which the AAV approximation holds) that the weak value can be arbitrarily large as the pre and post-selected states become orthogonal.

4. APPLICATIONS

We shall consider two applications of our exact treatment that may be of interest in quantum information. By using the entangled EPR-Bohm singlet state we point out an ambiguity that can arise if one uses AAV’s approach to encounter this type of situation which goes away if one considers exact treatment. In an another example we discuss the usefulness of the exact treatment in quantum games related to the issue of distinguishing differently prepared mixed state having same density matrix.

4.1. EPR-Bohm State and Ambiguities of the Usual Approach

Let us assume an EPR-Bohm singlet state as an initial state of a 2 particles system is

$$|\phi(t=0)\rangle = [|+\nu\rangle|-\nu\rangle - |-\nu\rangle|+\nu\rangle] |\psi^1\rangle|\psi^2\rangle, \quad (31)$$

where $|\psi^{1,2}\rangle$ are the spatial wavefunctions of particles 1 and 2, taken to be Gaussians with an initial momentum along opposite directions. Because of rotational invariance of the singlet state, the choice of ν can be taken to be arbitrary and the measurement results should not depend on that arbitrary choice.

Now consider the following setup. The source emits the particles at $t=0$ and they fly apart along two opposite directions. Alice makes a WM of a spin observable $\hat{\sigma}_a^1$ on particle 1 along the axis $\hat{\mathbf{a}}$ and Bob performs a WM of spin observable on particle 2 $\hat{\sigma}_b^2$ along some axis $\hat{\mathbf{b}}$. The wavefunction given by Eq. (31) becomes

$$|\phi(t>\tau)\rangle = \exp(-i\hat{\sigma}_a^1 \hat{x}^1) |+\nu\rangle |\psi^1\rangle \quad (32)$$

$$\otimes \exp(-i\hat{\sigma}_b^2 \hat{x}^2) |-\nu\rangle |\psi^2\rangle$$

$$- \exp(-i\hat{\sigma}_a^1 \hat{x}^1) |-\nu\rangle |\psi^1\rangle \otimes \exp(-i\hat{\sigma}_b^2 \hat{x}^2) |+\nu\rangle |\psi^2\rangle. \quad (33)$$

Finally, Alice and Bob post-select along $|u\rangle$ and $|w\rangle$ respectively. We shall now see the final pointer state by using both AAV formalism and our exact treatment.

4.1.1. Pointer wavefunction using AAV formalism.

After post-selection, following the method adopted in AAV formulation the post-selected pointer wavefunction can be written as

$$\begin{aligned} \langle u|\langle w|\phi(t>\tau)\rangle &= \langle u|+\nu\rangle\langle w|-\nu\rangle \\ &\times \exp\left(-i\hat{x}^1 \frac{\langle u|\hat{\sigma}_a^1|+\nu\rangle}{\langle u|+\nu\rangle}\right) |\psi^1\rangle \exp\left(-i\hat{x}^2 \frac{\langle w|\hat{\sigma}_b^2|-\nu\rangle}{\langle w|-\nu\rangle}\right) |\psi^2\rangle \\ &- \langle u|-\nu\rangle\langle w|+\nu\rangle \exp\left(-i\hat{x}^1 \frac{\langle u|\hat{\sigma}_a^1|-\nu\rangle}{\langle u|-\nu\rangle}\right) |\psi^1\rangle \\ &\times \exp\left(-i\hat{x}^2 \frac{\langle w|\hat{\sigma}_b^2|+\nu\rangle}{\langle w|+\nu\rangle}\right) |\psi^2\rangle. \end{aligned} \quad (34)$$

Now comes the crucial point. Since ν is arbitrary, we can in principle, choose $\nu = w$ so that Eq. (34) can be written as

$$\begin{aligned} \langle u|\langle w|\phi(t>\tau)\rangle &= -\langle u|-\nu\rangle \exp\left(-i\hat{x}^1 \frac{\langle u|\hat{\sigma}_a^1|-\nu\rangle}{\langle u|-\nu\rangle}\right) |\psi^1\rangle \\ &\times \exp\left(-i\hat{x}^2 \frac{\langle w|\hat{\sigma}_b^2|w\rangle}{\langle w|+\nu\rangle}\right) |\psi^2\rangle. \end{aligned} \quad (35)$$

Instead of choosing $v = w$ we could also take $v = u$, and in that case Eq. (34) is of the form

$$\begin{aligned} \langle u | \langle w | \phi(t > \tau) \rangle &= \langle w | -u \rangle \exp(-i\hat{x}^1 \langle u | \hat{\sigma}_a^1 | u \rangle) |\psi^1\rangle \\ &\times \exp\left(-i\hat{x}^2 \frac{\langle w | \hat{\sigma}_b^2 | -u \rangle}{\langle w | -u \rangle}\right) |\psi^2\rangle. \end{aligned} \quad (36)$$

The pointer behaviors according to Eqs. (35) and (36) are different, since according to Eq. (35) Alice's

pointer would indicate the weak value $\frac{\langle u | \hat{\sigma}_a^1 | -w \rangle}{\langle u | -w \rangle}$, and

Bob's pointer the mean value $\cos(w - b)$, whereas following Eq. (36). Alice's pointer would indicate $\cos(u - a)$ and Bob's measuring device would yield a

weak value $\frac{\langle w | \hat{\sigma}_b^2 | -u \rangle}{\langle w | -u \rangle}$. Of course, for choosing the

post-selected ensemble, Alice and Bob need to communicate (since Alice needs to know, for each event u that she registers, that Bob did obtain w), but the discrepancy between Eqs. (35) and (36) is relative to the *same* post-selected ensembles. This discrepancy will not arise if exact treatment is invoked instead of WM as given below.

4.1.2. Pointer wavefunction using exact treatment.

Let us now examine the above setup using our exact treatment. The first step in an exact treatment is to write the Eq. (31) in terms of the basis of $\hat{\sigma}_a^1$ and $\hat{\sigma}_b^1$. Writing Eq. (31) in those basis and rearranging we obtain

$$\begin{aligned} |\phi(t > \tau)\rangle &= \sin\left(\frac{b-a}{2}\right) \exp(-i\hat{\sigma}_a^1 \hat{x}^1) | +a \rangle |\psi^1\rangle \\ &\otimes \exp(-i\hat{\sigma}_b^2 \hat{x}^2) | +b \rangle |\psi^2\rangle \\ &+ \cos\left(\frac{b-a}{2}\right) \exp(-i\hat{\sigma}_a^1 \hat{x}^1) | +a \rangle |\psi^1\rangle \\ &\otimes \exp(-i\hat{\sigma}_b^2 \hat{x}^2) | -b \rangle |\psi^2\rangle \\ &- \cos\left(\frac{b-a}{2}\right) \exp(-i\hat{\sigma}_a^1 \hat{x}^1) | -a \rangle |\psi^1\rangle \\ &\otimes \exp(-i\hat{\sigma}_b^2 \hat{x}^2) | +b \rangle |\psi^2\rangle \\ &+ \sin\left(\frac{b-a}{2}\right) \exp(-i\hat{\sigma}_a^1 \hat{x}^1) | -a \rangle |\psi^1\rangle \\ &\otimes \exp(-i\hat{\sigma}_b^2 \hat{x}^2) | -b \rangle |\psi^2\rangle. \end{aligned} \quad (37)$$

Note that, this last expression does not depend on v . But, at this stage there is no point in applying the WM formalism—there are no more 'weak values' to compute in this last expression, in which the resolution of the identity in the WM basis was introduced, so that,

for example, $\exp(-i\hat{\sigma}_a^1 \hat{x}^1) | \pm a \rangle = \exp(\mp i\hat{x}^1) | \pm a \rangle$. Post-selecting on $|u\rangle$ and $|w\rangle$ we have

$$\begin{aligned} \langle u | \langle w | \phi(t > \tau) \rangle &= \langle u | +a \rangle \exp(-i\hat{x}^1) |\psi^1\rangle \\ &\times \left[\sin\left(\frac{b-a}{2}\right) \langle w | +b \rangle \exp(-i\hat{x}^2) |\psi^2\rangle \right. \\ &\quad \left. + \cos\left(\frac{b-a}{2}\right) \langle w | -b \rangle \exp(i\hat{x}^2) |\psi^2\rangle \right] \\ &+ \langle u | -a \rangle \exp(i\hat{x}^1) |\psi^1\rangle \left[-\cos\left(\frac{b-a}{2}\right) \langle w | +b \rangle \exp(-i\hat{x}^2) |\psi^2\rangle \right. \\ &\quad \left. + \sin\left(\frac{b-a}{2}\right) \langle w | -b \rangle \exp(i\hat{x}^2) |\psi^2\rangle \right]. \end{aligned} \quad (38)$$

Crucially, the post-selection yields an entangled state of the meters naturally expressed in the WM basis instead of separable state obtained using the standard WM techniques. Note that if Alice's measurement is ideal—in the sense that the momentum wavepackets obtained by the Fourier transform of $\exp(-i\hat{x}^1) |\psi^1\rangle$ and $\exp(i\hat{x}^1) |\psi^1\rangle$ do not overlap—she can correlate her meter with the WMs detected by Bob (alternatively she obtains the same by post-selecting along $u = \pm at$). Bob's WMs depend on a , something that is ambiguous if one employs the AAV formalism.

4.2. Quantum Games

Another illustration of the practical usefulness of the scheme employing exact weak values in a context of interest to quantum information tasks is in applications to quantum games [35]. Consider the following situation: Alice prepares neutral spin 1/2 particles in some state, either ρ_x or ρ_z and sends them to Bob, whose goal is to guess the state. According to elementary quantum mechanics the spin density matrices

$$\rho_x \equiv \frac{1}{2} |\uparrow_x\rangle \langle \uparrow_x| + \frac{1}{2} |\downarrow_x\rangle \langle \downarrow_x| \quad (39)$$

and

$$\rho_z \equiv \frac{1}{2} |\uparrow_z\rangle \langle \uparrow_z| + \frac{1}{2} |\downarrow_z\rangle \langle \downarrow_z| \quad (40)$$

are identical and thus undistinguishable. We impose an additional condition: we assume Alice sends successive spins of alternate signs, i.e., Alice sends either $\xi = \{|\uparrow_x\rangle, |\downarrow_x\rangle, |\uparrow_x\rangle, |\downarrow_x\rangle, \dots\}$ or $\zeta = \{|\uparrow_z\rangle, |\downarrow_z\rangle, |\uparrow_z\rangle, |\downarrow_z\rangle, \dots\}$, each of the sets ξ and ζ giving rise to a specific realization of ρ_x or ρ_z , respectively. Bob must guess as fast as possible, that is by processing the lowest number of particles, whether Alice is sending ξ or ζ .

With strong measurements, the best Bob can do is to measure either $\hat{\sigma}_x$ or $\hat{\sigma}_z$ and examine whether two successive measurements have identical signs. Sup-

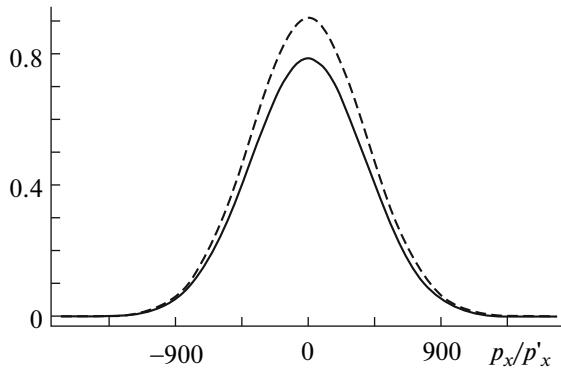


Fig. 4. Meter distribution (in arbitrary units) for a standard weak measurement of $\hat{\sigma}_x$ (see text). The solid (online red) curve corresponds to ξ , while the dashed (online blue) curve corresponds to ζ .

pose for instance Bob chooses to measure $\hat{\sigma}_x$; the pointer displays two sharp peaks, corresponding to positive and negative outcomes for the spin projection along x . Hence if ξ is sent the sign of successive outcomes will alternate, whereas if ζ is sent each outcome is equiprobable. So Bob's strategy will be to observe whether the consecutive measurements have alternating outcomes, in which case he will conclude it is likely Alice is sending ξ . Indeed denoting by k the number of particles that have already been seen to be displaying an alternate series, the probability of continuing with this series for the $(k + 1)$ th particle if ζ has been sent becomes 2^{-k} and decrease rapidly with k .

With standard weak measurements the problem for Bob is that he ignores the preselected state: he must guess whether Alice is sending ξ or ζ by obtaining meter distributions that are very broad in momentum space, irrespective of the weak measurement and post-selection Bob chooses. Typically all the meter distributions have almost identical profiles, but different heights, which is how ξ and ζ can be distinguished; an example is given in Fig. 4. So despite the fact that the meter distributions will indeed be different, in practice Bob will need a great number of particles in order to discriminate ξ from ζ .

However by following the exact treatment in the non-ideal case, Bob can set (by changing the SG magnetic field strength and passage time) the interference between the meter states in momentum space so that the detection of ξ and ζ result in probability distributions having distinct profiles (see Fig. 5). Moreover by weakening the coupling constant, Bob can still keep markedly different profiles in *momentum* space while obtaining non-overlapping profiles for the meter in *configuration* space. The advantage is obvious: one has exactly the same information as the one obtained with strong measurements (but in configuration space), and in addition as more particles are detected the

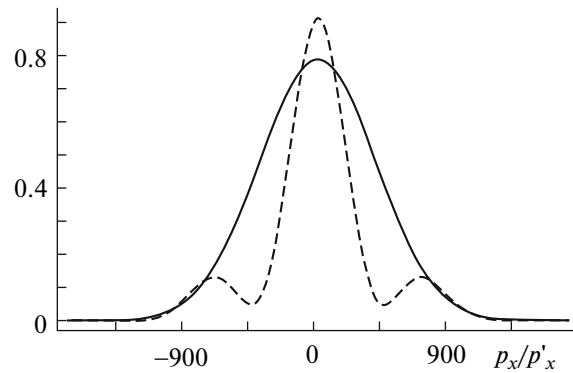


Fig. 5. Same as Fig. 4 but for an exact non-ideal measurement slightly away from the standard weak limit.

detection curve in momentum space unambiguously reveals whether ξ or ζ is being sent. It is crucial to note that the two distinctly positioned peaks visible in configuration space are a feature of the exact solutions—in the standard WM formalism the configuration space wavefunctions are identical up to some global factor.

In practice, each odd numbered result is registered separately from the even numbered events; this needs to be done simultaneously for both post-selected states. There are thus overall 4 registers (odd and even events register for each post-selected state) that count the number of events. When enough events are registered, simple statistical tests can be employed to fit the acquired data to one of the two curves. A typical example is shown in Fig. 6, corresponding to a numerical simulation of the game for a non-ideal measurement of $\hat{\sigma}_x$ followed by a post-selection along an angle $\theta = 235^\circ$. In the standard WM limit, Fig. 6a shows Bob's data acquisition for $N = 20$ odd events (generated randomly by computer simulation) along this post-selection angle when Alice has actually sent ξ . Figure 6b shows Bob's data acquisition for 20 odd events had Alice sent ζ . Bob must test the acquired data against the two theoretical curves shown in Fig. 4. For $N = 20$, it is not possible to discriminate between the two theoretical curves: assume Bob acquired the data shown in Fig. 6b; then the correct theoretical curve is the dashed blue line of Fig. 4. By performing a sum of squares analysis Bob cannot significantly discriminate between the two theoretical curves (the mean errors for the data acquired in Fig. 6b are 0.74 and 0.73 for the ξ and ζ curves, respectively). In the exact non-ideal case, the acquired data corresponding to Figs. 6a and 6b is shown in Figs. 6c and 6d, respectively. If we assume Bob has acquired the data shown in Fig. 6d, a comparison to the theoretical curves given in Fig. 5 is statistically significant: for the same number $N = 20$ of acquired events, testing the data against the solid red and dashed blue curves of Fig. 5 gives a mean error of 0.94 and 0.29, respectively. Note that to achieve an

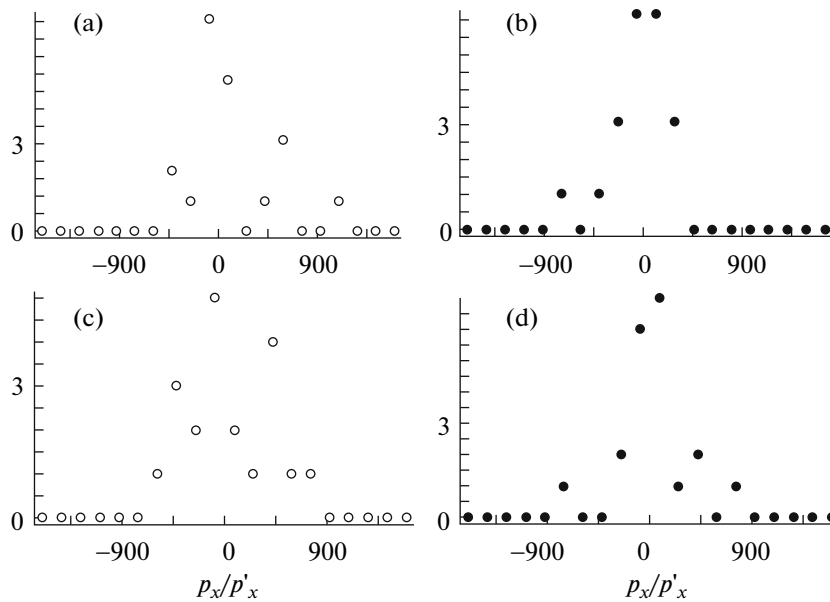


Fig. 6. Data acquired by Bob for $N = 20$ odd events in the standard WM limit (a, b) and for a non-ideal measurement (c, d) allowing Bob to achieve a better guess. (a, c): Data registered when Alice sends ξ . (b, d): Data registered when Alice sends ζ .

equivalent statistical significance in the standard WM case, a far greater number of events ($N \approx 500$) would be necessary.

5. SUMMARY AND CONCLUSIONS

By considering the differences between ideal and non-ideal measurements in both classical and quantum mechanics, we have introduced weak measurements as a specific instance of a non-ideal measurement followed by post-selection. This analysis sheds some light on the meaning of the weak measurement procedure, in particular the subtle point concerning the relation between the meter distribution and the measured system's properties. Based on an exactly solvable problem of the spin measurement in Stern-Gerlach setups, we have investigated with exact solutions the weak, strong and the intermediate non-ideal measurement regimes. We have defined “semiweak” values that can be larger than the standard weak values, as well as “exact weak values” that can be obtained in cases in which the usual AAV formalism breaks down (such as for orthogonal pre and post-selected states). We have further seen that some ambiguities present in the standard WM formalism can be avoided with the exact treatment, and discussed the example of a quantum game that can be played more advantageously with non-ideal rules rather than by performing weak or ideal measurements.

REFERENCES

1. Y. Aharonov, D. Z. Albert, and L. Vaidman, *Phys. Rev. Lett.* **60**, 1351 (1988).
2. Y. Aharonov and L. Vaidman, *J. Phys., Ser. A* **24**, 2315 (1991).
3. L. Vaidman, *Found. Phys.* **26**, 895 (1996).
4. Y. Aharonov and A. Botero, *Phys. Rev., Ser. A* **72**, 052111 (2005).
5. G. Mitchison, R. Jozsa, and S. Popescu, *Phys. Rev., Ser. A* **76**, 060302 (2007).
6. J. Tollaksen, *J. Phys., Ser. A* **40**, 9033 (2007).
7. R. Jozsa, *Phys. Rev., Ser. A* **76**, 044103 (2007).
8. N. S. Williams and A. N. Jordan, *Phys. Rev. Lett.* **100**, 026804 (2008).
9. S. Wu and Y. Li, *Phys. Rev., Ser. A* **83**, 052106 (2011).
10. K. Nakamura, A. Nishizawa, and M. K. Fujimoto, *Phys. Rev., Ser. A* **85**, 012113 (2012).
11. A. K. Pan and A. Matzkin, *Phys. Rev., Ser. A* **85**, 022122 (2012).
12. Y. Shikano, in *Measurements in Quantum Mechanics*, Ed. by M. R. Pahlavani (InTech, 2012), Ch. 4.
13. I. M. Duck, P. M. Stevenson, and E. C. G. Sudarshan, *Phys. Rev., Ser. D* **40**, 2112 (1989).
14. N. W. M. Ritchie, J. G. Story, and R. G. Hulet, *Phys. Rev. Lett.* **66**, 1107 (1991).
15. Q. Wang, F. W. Sun, Y. S. Zhang, et al., *Phys. Rev., Ser. A* **73**, 023814 (2006).
16. G. L. Pryde, J. L. O'Brien, A. G. White, et al., *Phys. Rev. Lett.* **94**, 220405 (2008).
17. O. Hosten and P. Kwiat, *Science* **319**, 787 (2008).
18. K. Yokota, T. Yamamoto, M. Koashi, and N. Imoto, *New J. Phys.* **11**, 033011 (2009).
19. D. J. Starling, P. B. Dixon, A. N. Jordan, and J. C. Howell, *Phys. Rev., Ser. A* **80**, 041803(R) (2009).
20. P. B. Dixon, D. J. Starling, A. N. Jordan, and J. C. Howell, *Phys. Rev. Lett.* **102**, 173601 (2009).

21. O. Zilberberg, A. Romito, and Y. Gefen, *Phys. Rev. Lett.* **106**, 080405 (2011).
22. S. Kocsis, B. Braverman, S. Ravets, et al., *Science* **332**, 117 (2011).
23. A. Peres, *Quantum Theory: Concepts and Methods* (Kluwer, Dordrecht, 1993).
24. P. E. Toschek and C. Balzer, *Laser Phys.* **12**, 253 (2002).
25. I. B. Mekhov and H. Ritsch, *Laser Phys.* **21**, 1486 (2011).
26. A. Matzkin, *Eur. J. Phys.* **23**, 285 (2002).
27. D. N. Klyshko, *Laser Phys.* **8**, 363 (1998).
28. A. Bassi and G. Ghirardi, *379*, 257 (2003).
29. N. Bohr, *Atomic Physics and Human Knowledge* (Wiley, New York, USA, 1958).
30. W. H. Zurek, *Rev. Mod. Phys.* **75**, 715 (2003).
31. D. Bohm, *Phys. Rev.* **85**, 166 (1952); *ibid.* **85**, 180 (1952); D. Bohm and B. J. Hiley, *The Undivided Universe* (Routledge, London, 1993).
32. H. D. Zeh, *Found. Phys.* **40**, 1476 (2010).
33. Y. Aharonov, P. G. Bergmann, and J. L. Lebowitz, *Phys. Rev., Ser. B* **134**, 1410 (1964).
34. D. Home, A. K. Pan, M. M. Ali, and A. S. Majumdar, *J. Phys., Ser. A* **40**, 13975 (2007); D. Home and A. K. Pan, *J. Phys., Ser. A* **42**, 165302 (2009).
35. J. Volz, M. Weber, D. Schlenk, et al., *Laser Phys.* **17**, 1007 (2007).